Int J Thermophys (2009) 30:1578–1590
DOI 10.1007/s10765-009-0630-2

Density and Volume Fraction of Supercritical CO_2 in Pores of Native and Oxidized Aerogels

Y. B. Melnichenko · G. D. Wignall

Received: 2 October 2008 / Accepted: 20 July 2009 / Published online: 4 August 2009

Abstract The density and volume fraction of an adsorbed phase of carbon dioxide (CO_2) in aerogels was investigated using a formalism based on independent measurements of neutron transmission and small-angle neutron scattering from fluid-saturated absorbers (Rother et al. J. Phys. Chem. C **111**, 15736 (2007)). The range of excess fluid pressures ($0 < P < 8\,\text{MPa}$) and temperatures ($T = 35\,°\text{C}$ and $80\,°\text{C}$) corresponded to the supercritical regime above the critical temperature $T_C = 31.1\,°\text{C}$ and critical density $\rho_C = 0.468\,\text{g}\cdot\text{cm}^{-3}$ of the bulk fluid. The results demonstrate that a porous aerogel matrix works to create an adsorbed phase with liquid-like fluid densities reaching $\sim 1.1\,\text{g}\cdot\text{cm}^{-3}$ and $\sim 0.8\,\text{g}\cdot\text{cm}^{-3}$ at $T = 35\,°\text{C}$ and $80\,°\text{C}$, respectively. Thus, despite the fact that the density and volume fraction of the adsorbed fluid both decrease with temperature, the dense adsorbed phase is still present in the aerogel at temperatures far exceeding the T_C. Heat treatment ("oxidation") of the aerogel at 500 °C for 2 h, which removes a significant fraction of the alkyl groups from the aerogel surface, has little effect on the adsorption properties. The observed reduction of the density and volume fraction of the adsorbed CO_2 with temperature and its minor dependence on the surface modification are consistent with predictions of the pore-filling model.

Keywords Adsorption · Aerogels · Carbon dioxide · Small-angle neutron scattering

1 Introduction

Carbon dioxide (CO_2) emissions from anthropogenic sources are frequently directly linked to the rising level of atmospheric CO_2 and to global warming [1]. Carbon

---

Y. B. Melnichenko (✉) · G. D. Wignall
Neutron Scattering Sciences Division, Oak Ridge National Laboratory,
Oak Ridge, TN 37831-6393 USA
e-mail: melnichenkoy@ornl.gov

capture and sequestration in underground natural porous media (saline aquifers, depleted oil, and gas reservoirs as well as unmineable coal seams) are a proposed measure for arresting the rising concentration of atmospheric carbon dioxide. Sequestration of CO_2 in unmineable deep coal seams is particularly attractive due to the relatively high sorption capacity exhibited by coal as well as the proximity of geological sites potentially suitable for geological storage to coal-burning power plants which generate roughly one-third of the United States' CO_2 emissions. The amount of CO_2 that is expected to be adsorbed by a specific coal is one of the critical parameters for sequestration technology. In addition to the petrographic composition, the sorption capacity of coal depends on the seam depth which defines the temperature (T) and pressure (P) at which CO_2 will be adsorbed after injection. Traditionally the sorption capacity of coal and other porous adsorbers at different (T, P) has been studied using measurements of sorption isotherms or mercury porosimetry. However, none of the existing experimental methods alone is able to provide all the necessary information needed to understand and predict fluid adsorption capacities in various porous materials. For this reason, it is important to develop and refine the scattering techniques and their interpretations as a reliable tool for probing adsorption properties of sub- and super-critical fluids in porous systems with different geometries.

Coal is chemically and structurally an inhomogeneous natural porous material, and accurate interpretation of the scattering from CO_2-saturated coals requires preliminary studies of the fluid adsorption in model porous systems with known and simple chemical composition as well as a well-characterized porous structure, such as aerogels. Evaluation of the adsorption properties on an absolute scale requires information on the density (ρ_a) and volume fraction (ϕ_a) of the adsorbed phase, which was not readily accessible by existing techniques. A method of determination of (ρ_a) and (ϕ_a) was developed and applied by Rother et al. [2] who showed that both parameters may be determined via combined measurements of neutron transmission and small-angle neutron scattering (SANS) from fluid-saturated porous absorbers. This formalism was applied to characterize adsorption properties of deuterated propane in silica aerogels. It was also applied to calculate ρ_a and ϕ_a of CO_2 in a similar aerogel at $T = 35\,^{\circ}\mathrm{C}$ using data collected by Melnichenko et al. [3], which had been previously analyzed in terms of the excess adsorption.

The approach described in [2] utilizes the theory of scattering from three-phase systems initially developed by Wu [4] to model scattering from microvoids in binary composite materials, which involves subtraction of the scattering invariant from a hypothetical two-phase system. In this article, we revisit the theory of Wu and demonstrate that the parameters of the adsorbed phase (ρ_a, ϕ_a) can be determined from neutron transmission and scattering data without calculating and subtracting the two-phase invariant, Z_0, which in this case represents an absorber homogeneously saturated with the unadsorbed fluid. For the case of significant fluid adsorption, Z_0 can not be measured experimentally and was previously calculated based on the equation of state of the bulk fluid [2]. We also present a modified expression for the neutron contrast factor of a three-phase system, which allows for finding a direct solution of the equation for the invariant of the three-phase system Z against, e.g., the volume fraction of the adsorbed phase. Along with the avoided calculation and subtraction of Z_0, this significantly simplifies computations.

The new formulae are used to calculate the density and volume fraction of the adsorbed phase of CO_2 in aerogels using data [3] previously analyzed in terms of the excess adsorption parameter. The obtained results are compared with the adsorption behavior of deuterated propane in similar aerogels as well as with the predictions of the pore-filling model.

2 Neutron Contrast and the Invariant of Three-Phase Systems

Consider a system with the total volume V_t which consists of three "phases": solid porous material, unadsorbed fluid in the pore center (the molecules of which do not interact with the pore walls), and adsorbed fluid with the volumes V_s, V_u, and V_a, respectively,

$$V_\mathrm{t} = V_\mathrm{s} + V_\mathrm{u} + V_\mathrm{a} = V_\mathrm{s} + V_\mathrm{p} \tag{1}$$

where $V_\mathrm{p} = V_\mathrm{u} + V_\mathrm{a}$ is the pore volume accessible to the unadsorbed and adsorbed fluid. The volume fraction of phase i is $\phi_i = V_i / V_\mathrm{t}$ and, therefore,

$$\phi_\mathrm{s} + \phi_\mathrm{u} + \phi_\mathrm{a} = 1. \tag{2}$$

The neutron coherent cross-section $I(Q)$ in units of cm^{-1} of the three-phase system is proportional to the fluctuations of the neutron scattering length density (neutron contrast κ_n) [5–7]

$$I(Q) \sim \kappa_\mathrm{n} \equiv \frac{1}{V} \int\limits_{v} \rho *^2 (r)\, \mathrm{d}v = \sum_{1 \leq i < j \leq 3} (\rho_i^* - \rho_j^*)^2 \phi_i \phi_j \tag{3}$$

where ρ_i^* is the scattering length density of phase i. Based on Eq. 3, Wu [4] calculated the scattering invariant Z of a three-phase system:

$$\begin{aligned} Z &= \int_0^\infty Q^2 I(Q) \mathrm{d}Q = 2\pi^2 \kappa_\mathrm{n} \\ &= 2\pi^2 \left[(\rho_\mathrm{s}^* - \rho_\mathrm{u}^*)^2 \phi_\mathrm{s}\phi_\mathrm{u} + (\rho_\mathrm{u}^* - \rho_\mathrm{a}^*)^2 \phi_\mathrm{u}\phi_\mathrm{a} + (\rho_\mathrm{s}^* - \rho_\mathrm{a}^*)^2 \phi_\mathrm{s}\phi_\mathrm{a} \right] \end{aligned} \tag{4}$$

As mentioned above, this expression was originally developed to model scattering from microvoids in binary composite materials, but can also be applied to analyze scattering from gases adsorbed in porous media [2,3], where the adsorbed phase takes the place of the microvoids in the original formulation. In the case of zero adsorption ($\phi_\mathrm{a} = 0$), Eq. 4 reduces to the well-known expression for the neutron invariant of a two-phase system [8];

$$Z_0 = \int\limits_0^\infty Q^2 I(Q) \mathrm{d}Q = 2\pi^2 \phi_\mathrm{s} (1 - \phi_\mathrm{s}) (\rho_\mathrm{s}^* - \rho_\mathrm{u}^*)^2 \tag{5}$$

Combining Eqs. 4 and 5, Wu derived an equation for the volume fraction of the third phase

$$\phi_{\mathrm{a}} = \frac{Z - Z_0}{2\pi^2 \left[\phi_{\mathrm{u}}(\rho_{\mathrm{u}}^* - \rho_{\mathrm{a}}^*)^2 + \phi_{\mathrm{s}}(\rho_{\mathrm{s}}^* - \rho_{\mathrm{a}}^*)^2 - \phi_{\mathrm{s}}(\rho_{\mathrm{s}}^* - \rho_{\mathrm{u}}^*)^2\right]}. \tag{6}$$

The application of Eq. 6 in conjunction with neutron transmission data requires calculation of the invariant of the hypothetical two-phase system Z_0 (Eq. 5), which was previously conducted using the equation of state of the fluid [2]. Analysis of Eq. 4, however, shows that this procedure may be avoided by eliminating the volume fraction of the adsorbed phase ϕ_{a} in the right-hand side of Eq. 4 using Eq. 2 which leads to

$$\begin{aligned} Z &= \int_0^\infty Q^2 I(Q)\mathrm{d}Q = 2\pi^2 \kappa_{\mathrm{n}} \\ &= 2\pi^2 \Big[(\rho_{\mathrm{s}}^* - \rho_{\mathrm{a}}^*)^2 \phi_{\mathrm{s}}(1-\phi_{\mathrm{s}}) \\ &\quad + (\rho_{\mathrm{u}}^* - \rho_{\mathrm{a}}^*)^2 \phi_{\mathrm{u}}(1-\phi_{\mathrm{u}}) - 2(\rho_{\mathrm{s}}^* - \rho_{\mathrm{a}}^*)(\rho_{\mathrm{u}}^* - \rho_{\mathrm{a}}^*)\phi_{\mathrm{s}}\phi_{\mathrm{u}}\Big] \end{aligned} \tag{7}$$

The quadratic Eq. 7 may be solved against the volume fraction of the undsorbed phase[1]:

$$\phi_{\mathrm{u}} = \frac{-b - \sqrt{b^2 - 4ac}}{2a} \tag{8}$$

where

$$\begin{aligned} a &\equiv (\rho_{\mathrm{u}}^* - \rho_{\mathrm{a}}^*)^2, \\ b &\equiv 2(\rho_{\mathrm{s}}^* - \rho_{\mathrm{a}}^*)(\rho_{\mathrm{u}}^* - \rho_{\mathrm{a}}^*)\phi_s - (\rho_{\mathrm{u}}^* - \rho_{\mathrm{a}}^*)^2, \\ c &\equiv Z/2\pi^2 - (\rho_{\mathrm{s}}^* - \rho_{\mathrm{a}}^*)^2 \phi_{\mathrm{s}}(1-\phi_{\mathrm{s}}) \end{aligned} \tag{9}$$

Equation 8 may be supplemented by an additional equation that relates ϕ_{u} with the average pore density ρ_{p} (see Eqs. 5 and 6 in [2]). As explained in [2], the latter parameter may be independently determined based on the neutron transmission measurements from the fluid-saturated absorber at different temperatures and pressures. Because of reasons outlined in the Appendix, we use the following relation between ϕ_{u} and ρ_{p}, in place of Eq. 6 in Ref. [2]:

$$\phi_{\mathrm{u}} = \frac{\rho_{\mathrm{a,p}}(1-\phi_{\mathrm{s}}) - \rho_{\mathrm{p}}}{\rho_{\mathrm{a,p}} - \rho_{\mathrm{u,p}}} \tag{10}$$

where $\rho_{\mathrm{a,p}}$ and $\rho_{\mathrm{u,p}}$ are the densities of the adsorbed and unadsorbed fluid phases *inside and accessible to the fluid pore volume* V_{p}. Equations 8 and 10 can be solved

---

[1] The root $\phi_{\mathrm{u}} = (-b + \sqrt{b^2 - 4ac})/2a$ of Eq. 8 produces unphysical values of $\phi_{\mathrm{u}} > 1$.

numerically by finding the value of ρ_a at which both of them are satisfied simultaneously. This provides values of the density and volume fraction of the adsorbed phase at a specific temperature and pressure.

3 Experimental

Base-catalyzed silica aerogels with a nominal density $\rho_{\text{aerogel}} = 0.1\,\text{g} \cdot \text{cm}^{-3}$, corresponding to $\sim$96 % porosity ($\phi_s = 0.04$), were obtained from Oscellus Technologies, Livermore, CA. The aerogels consist of thin silica strands with an average mesh size of 60 Å to 70 Å [9]. The aerogels were shaped into cylinders which fit tightly in the internal volume of the cell. The cell was pressurized with CO_2 (Matheson Gas Products, Inc, SFC purity 99.99 %) using a screw-type pressure generator. At each new pressure, the aerogel samples were equilibrated for $\sim$10 min to ensure completion of the formation of the adsorbed phase and equilibrium between the pressure of the unadsorbed fluid in the pore center and the external pressure in the pressure generator. The pressure at each temperature was measured using a precision digital indicator, and the fluid density was calculated at each pressure/temperature combination using NIST-12 software (http://www.nist.gov/srd/nist12.htm). The surface of native (nonoxidized) aerogels is covered by abundant methoxy groups (=Si–O–CH_3), which can be removed by heating the aerogel to $\sim$500 °C for 2 h, and this process is referred to as "oxidation" [9]. The experiments were performed with two aerogel samples, one of them was heat treated (oxidized) and the other in its original, as received, (nonoxidized) state.

Small-angle neutron scattering experiments were performed on the KWS-2 SANS facility at the FRJ2 reactor in Jülich, Germany. The neutron wavelength was $\lambda = 6.3$ Å ($\Delta\lambda/\lambda = 0.10\,\%$). The scattering from confined CO_2 was measured in the range of scattering vectors $Q = 4\pi\lambda^{-1}\sin\theta(0.01\,\text{Å}^{-1} < Q < 0.07\,\text{Å}^{-1})$, where 2θ is the scattering angle. The transmission at each pressure and temperature was measured continuously in situ using a He^3 straight beam monitor. The SANS datasets were corrected for instrumental backgrounds and normalized to an absolute differential cross-section per unit sample volume [$I(Q)$ in units of cm^{-1}] by means of pre-calibrated secondary standards [10].

4 Results and Discussion

The neutron transmission of CO_2-saturated oxidized and nonoxidized aerogels at pressures, corresponding to the bulk fluid density $\rho_{CO_2} < 0.5\,\text{g} \cdot \text{cm}^{-3}$ is shown in Fig. 1 along with the transmission of bulk CO_2. As discussed in [3], the strong negative deviation of the transmission of CO_2-saturated aerogel from that of bulk CO_2 indicates formation of a dense adsorbed fluid phase with a density higher than that of bulk CO_2 at the same thermodynamic conditions. Figure 2 shows the variation of the average fluid density in pores determined from the measured transmission using Eqs. A1 and A4. As is seen, the average density of CO_2 in pores much exceeds the density of the bulk fluid at the same thermodynamic conditions at both $T = 35\,°\text{C}$ and 80 °C; however, ρ_p at $T = 35\,°\text{C}$ is approximately a factor of two higher than ρ_p at $T = 80\,°\text{C} \gg T_C$

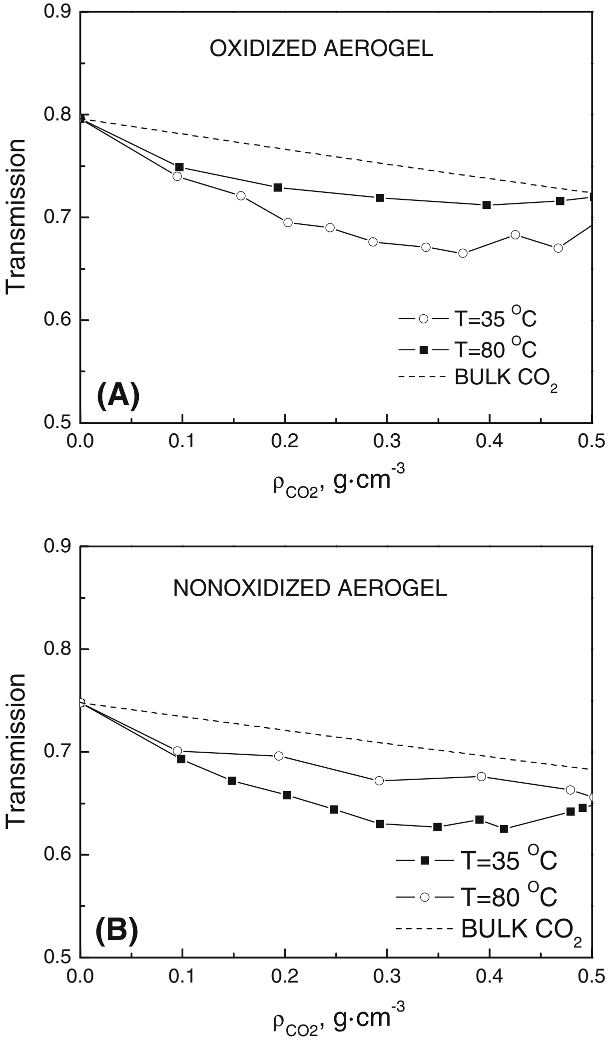

Fig. 1 Transmission of (**a**) oxidized and (**b**) nonoxidized aerogel versus density of CO_2 at two temperatures specified in the *inset*. *Dashed lines* represent transmission of bulk CO_2

due to closer proximity to the gas–liquid critical point. Figure 3 shows the scattering invariant calculated from the neutron cross-section $I(Q)$ at different pressures and temperatures using a procedure described in [3]. Similarly to ρ_p, the values of Z at $T = 35\,°C$ exceed those of Z at $T = 80\,°C$, which is due to the increasing scattering length density fluctuations as $T \Rightarrow T_C$.

The values of ρ_p calculated from neutron transmission, Z obtained from SANS measurements, $\phi_s = 0.04$, $\rho_s^* = 3.16 \times 10^{10}\,cm^{-2}$ [3], as well as the mass and scattering length densities ρ_u, ρ_u^* calculated using the equation of state of CO_2 (http://www.nist.gov/srd/nist12.htm), were substituted in Eqs. 8 and 10, which were numerically solved at each pressure and temperature following the routine outlined above.

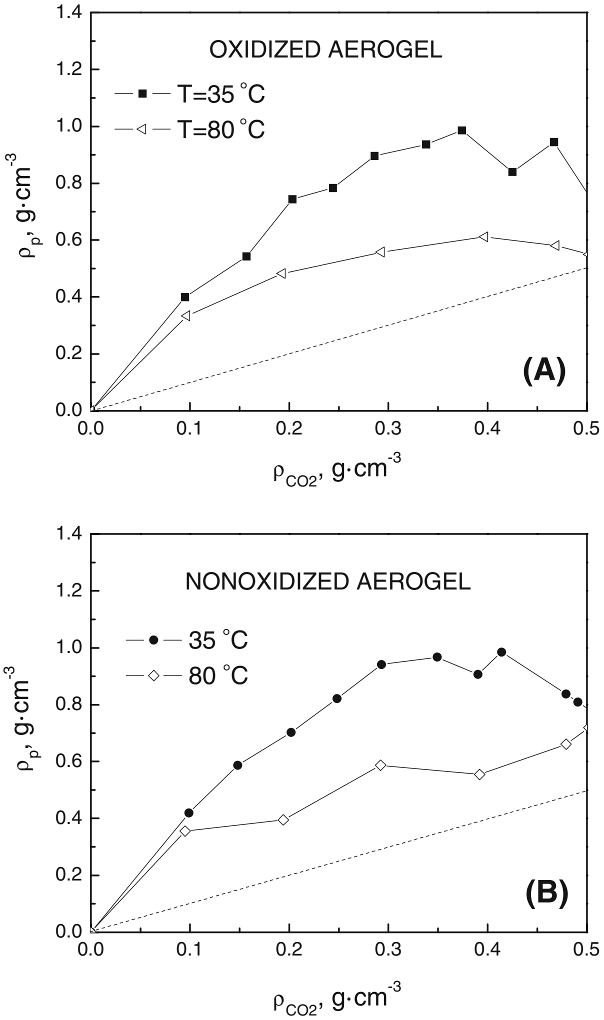

Fig. 2 Average density of CO_2 in pores of (**a**) oxidized and (**b**) nonoxidized aerogel versus density of CO_2 at two temperatures specified in the *inset*; obtained from the transmission data shown in Fig. 1 using Eqs. A1 and A4. *Dashed line* is described by equation $\rho_p = \rho_{CO_2}$

The values of the density ρ_a and volume fraction ϕ_a of the adsorbed phase thus obtained are shown in Figs. 4 and 5, respectively. The data confirm previous conclusions [2,3] on the formation of the adsorbed fluid phase in fluid-saturated aerogels with the density much exceeding that of the unadsorbed (bulk) fluid at similar thermodynamic conditions. For an oxidized aerogel, the calculated density $\rho_a = 1.12\,\text{g} \cdot \text{cm}^{-3}$ and volume fraction $\phi_a = 0.82$ of the adsorbed phase are in good agreement with previous estimates based on SANS measurements ($\rho_a = 1.07\,\text{g}\cdot\text{cm}^{-3}$, $\phi_a = 0.78$, respectively) [3,11]. The measured values of ρ_a are consistent with high densities of the adsorbed phase reported for CO_2 adsorbed in activated carbon with an average pore size of 17 Å

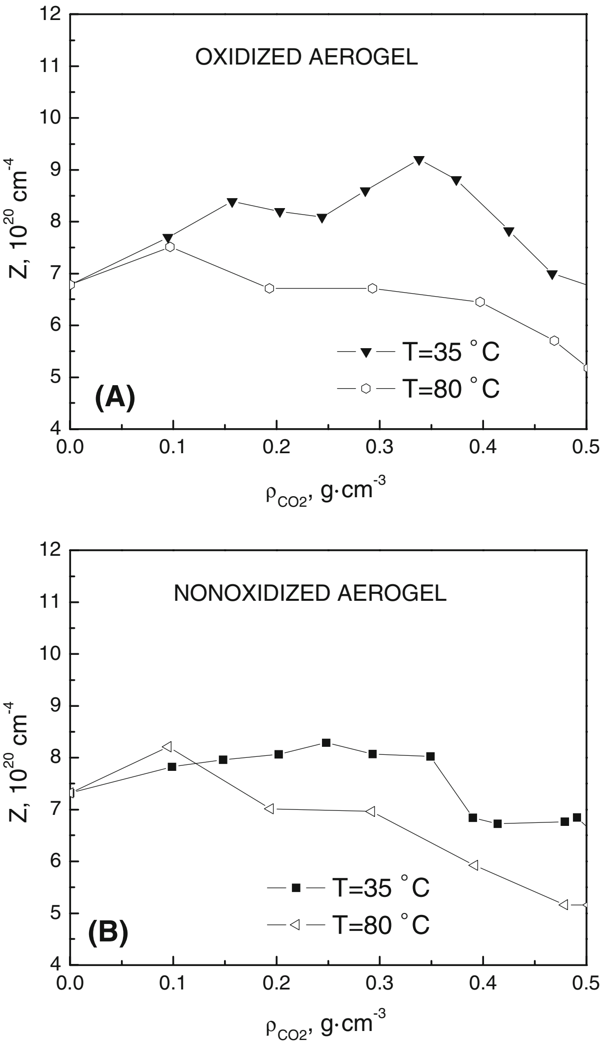

Fig. 3 Scattering invariant of (**a**) oxidized and (**b**) nonoxidized aerogel at two temperatures specified in the *inset*

($\rho_a \sim 1.03\,\mathrm{g\cdot cm^{-3}}$) [12] as well as in NaY zeolite with pore sizes in the range of 25 Å ($\rho_a \sim 1.27\,\mathrm{g\cdot cm^{-3}}$) [13]. The formation of an adsorbed CO_2 phase with a density far exceeding that of the bulk fluid ($\rho_a \geq 1.1\,\mathrm{g\cdot cm^{-3}}$) was documented in porous silica with pore diameters in the range from 20 Å to 150 Å by Schneider et al. [14] using Fourier transform infrared (FTIR) spectroscopy. Evidence for the formation of densified CO_2 layers formed in microporous carbon at near-critical conditions was provided by means of neutron powder diffraction (Steriotis et al. [15,16]) and repeatedly demonstrated in experiments by Chan and co-workers [17–19] and Herman and Beamish [20–22].

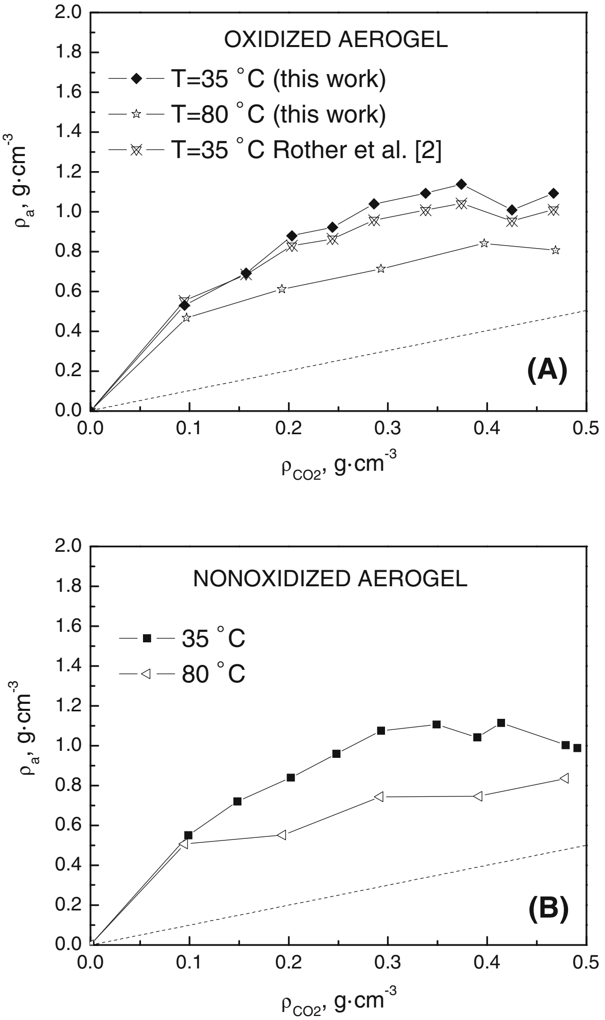

Fig. 4 Density of the adsorbed phase in pores of (**a**) oxidized and (**b**) nonoxidized aerogel at two temperatures specified in the *inset*. Figure 4a shows the results of calculations of ρ_a by Rother et al. [2]. *Dashed line* is described by equation $\rho_a = \rho_{CO_2}$

Our data show that the dense adsorbed phase of CO_2 in aerogels is formed not only in the proximity of the gas–liquid critical point but also at temperatures exceeding T_C by ~50 °C. At $T = 80\,°C$, the values of ρ_a and ϕ_a are 20 % to 30 % lower than corresponding values at $T = 35\,°C$, which underlines the importance of the proximity to the gas–liquid critical point in the physical properties of the adsorbed fluid phase. The observed decrease of the density and volume fraction of the adsorbed CO_2 with temperature is consistent with the pore-filling model for supercritical fluids [23] which assumes that there is a characteristic pore size below which the pores are uniformly filled with the high-density adsorbed phase and above which, the fluid is characterized

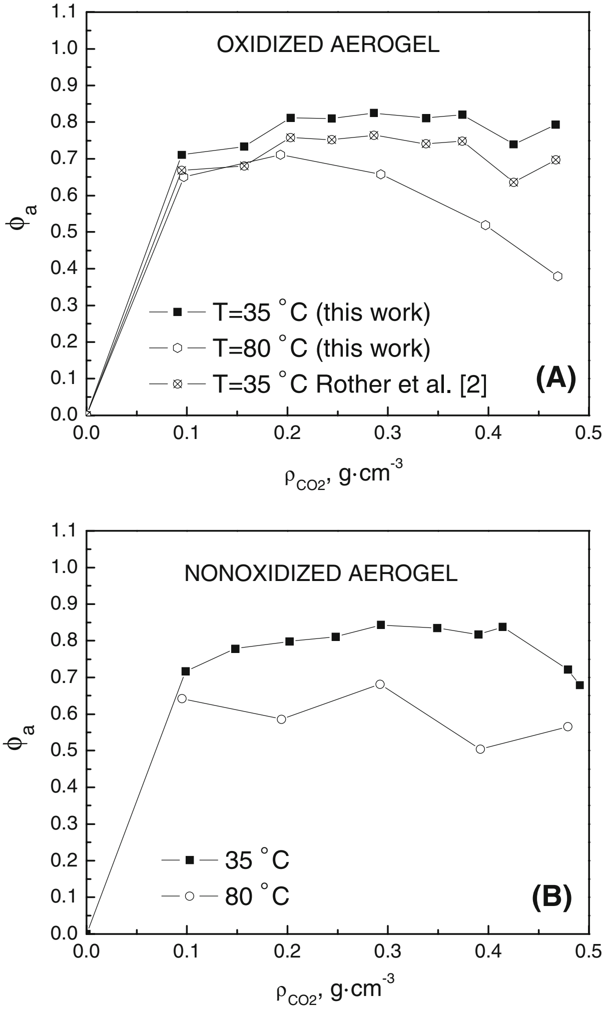

Fig. 5 Volume fraction of the adsorbed phase in (**a**) oxidized and (**b**) nonoxidized aerogel at two temperatures specified in the *inset*. Figure 5a shows the results of calculations of ϕ_a by Rother et al. [2]

by high density near the pore surface and lower density away from it. As the temperature increases, so does the kinetic energy of the fluid molecules, which means that only increasingly small pores can be completely filled by the adsorbed fluid molecules. This should result in a lower average density and volume of the adsorbed phase and thus a lower sorption capacity at higher temperatures, and this prediction correlates well with our observations.

Test calculations conducted using a combination of Wu's Eq. 6 and our Eq. 10 have produced values of ρ_a and ϕ_a indistinguishable within experimental error from ρ_a and ϕ_a obtained using a combination of Eqs. 8 and 10, which confirms self-consistency of the proposed method. Figures 4 and 5 also show the variation of ρ_a and ϕ_a generated by our proposed new formalism, and also by previous calculations [2] for CO_2-saturated oxidized aerogels at $T = 35\,°C$. The results are broadly consistent, with the differences in the range of 10 % to 15 % over the whole range of densities.

5 Conclusions

In this article, we presented a refined method of determination of the density and volume fraction of the adsorbed fluid phase based on a modified relation between the scattering invariant and neutron contrast of the three-phase systems. The advantage of the proposed Eqs. 7–9 is the eliminated necessity of calculation and subtraction of the invariant of a hypothetical two-phase system (absorber homogeneously saturated with unadsorbed fluid), and the availability of the direct solution of Eq. 7, which significantly simplifies calculations.

Using the developed methodology, we revisited experimental data on neutron transmission and SANS from CO_2-saturated oxidized and nonoxidized aerogels [3] and analyzed the variation of the density and volume fraction of the adsorbed CO_2 at temperatures close and far away from the liquid–gas critical temperature of the bulk fluid. The observed decrease of the density and volume fraction of the adsorbed CO_2 with temperature is consistent with the predictions of the pore-filling model for supercritical fluids [23] as well as with experimental data on adsorption of CO_2 and methane in coals and activated carbons [24]. Removal of the alkyl groups from the aerogel surface via oxidation has a negligible effect on the measured values of ρ_a and ϕ_a both close and far away from the critical temperature. This leads us to a conclusion that the adsorption of supercritical CO_2 in aerogels is governed predominantly by long-range van der Waals interactions between the silica skeleton of the aerogels and fluid molecules. Because of comparable values of ρ_a and ϕ_a close and far away from the critical point, we speculate that the range of these forces is comparable to the dimension of pores corresponding to the maximum of the aerogel pore-size distribution (∼60–70 Å).

The described methodology can be applied for handling and interpretation of SANS and ultra-SANS (USANS) data from CO_2-saturated coals, sandstones, shales, and other natural porous materials of interest for CO_2 sequestration at temperatures and pressures similar to underground conditions [25,26]. We believe that it may also be of interest for studies of the preferential adsorption from fluid mixtures (e.g., methane—CO_2) as well as for other fluid adsorption-related technologies such as gas separation and storage, catalysis, and supercritical extraction [27].

Acknowledgments The authors wish to thank H. Frielinghaus for his help during SANS experiments and also W. L. Wu for careful reading of the manuscript and helpful remarks. This research was sponsored by the Laboratory Directed Research and Development Program and by the Division of Materials Sciences, Office of Basic Energy Sciences, U. S. Department of Energy under Contract No. DE-AC05-00OR22725, Oak Ridge National Laboratory, managed by UT-Battelle, LLC.

Appendix

Here, we will discuss the advantage of Eq. 10 versus Eq. 6 in [2] for calculation of the density ρ_a and volume fraction ϕ_a of the adsorbed fluid phase in solid absorbers. The total neutron transmission of the three-phase system T is defined as the ratio of the intensity (I) transmitted through the sample, compared to that of the incident beam (I_O) [2,4]:

$$T = \frac{I}{I_0} = T_1 \exp(-\overline{\rho}_t C d) \tag{A1}$$

where T_1 is the transmission of an empty absorber, constant $C = N_{Av}\sigma/M$, N_{Av} is the Avogadro number, σ is the total neutron cross section of the atoms of the adsorbed fluid, M is the molar mass of the saturating fluid, and d is the total sample thickness. $\overline{\rho}_t$ is the average density of the unadsorbed and adsorbed fluid in the sample, i.e., the density, normalized to the total sample volume V_t:

$$\overline{\rho}_t = \frac{m_u}{V_t} + \frac{m_a}{V_t} = \rho_{u,t}\phi_u + \rho_{a,t}\phi_a \tag{A2}$$

where $m_u = \rho_u V_u$ and $m_a = \rho_a V_a$ are the masses and $\phi_u = V_u/V_t$ and $\phi_a = V_a/V_t$ are the volume fractions of the unadsorbed and adsorbed phases, respectively. Depending on the absorber porosity, different samples with the same total volume may have a different pore volume (V_p) accessible to the saturating fluid, and thus the average density $\overline{\rho}_t$ in Eq. A2 is a sample-specific parameter which has little physical meaning. The variable of interest is the average density of the fluid in the pores, i.e., the density normalized to the pore volume V_p:

$$\rho_p = \frac{m_u}{V_p} + \frac{m_a}{V_p} \equiv (\rho_{u,p}\phi_u + \rho_{a,p}\phi_a) \tag{A3}$$

which defines the average density *in pores* free from dependence of the absorber porosity. Taking into account that $V_p = V_t - V_s = V_t(1-\phi_s)$, we obtain from Eqs. A2 and A3,

$$\rho_p = (\rho_{u,p}\phi_u + \rho_{a,p}\phi_a) = \overline{\rho_t}/(1-\phi_s) \tag{A4}$$

Equation A4 between ρ_p and $\overline{\rho}_t$ was first introduced in [2]. It is important to emphasize, however, that Eq. 6 in [2] was derived using *total fluid densities*. In our notations it reads

$$\phi_u = \frac{\rho_{a,t} - \rho_p}{\rho_{a,t} - \rho_{u,t}}(1-\phi_s). \tag{A5}$$

Thus, to obtain correct values of ϕ_u from Eq. A5, the values of the adsorbed ($\rho_{a,p}$) and unadsorbed ($\rho_{u,p}$) fluid densities in pores should be converted into the total average densities ($\rho_{a,t}$) ($\rho_{u,t}$) by multiplying ($\rho_{a,p}$), ($\rho_{u,p}$) by a factor of $(1-\phi_s)$. This unnecessary procedure may be avoided by calculating ϕ_u via $\rho_{a,p}$ and $\rho_{u,p}$ directly using Eq. 10 which was applied in this article to analyze the behavior of the adsorbed density and volume fraction of CO_2 in aerogels, as described in the text.

References

1. Working Group III of the Intergovernmental Panel on Climate Change, in *IPCC Special report on carbon dioxide capture and storage*, ed. by B. Metz, O. Davidson, H.C. de Connick, M. Loos, L.A. Meyer (Cambridge University Press, Cambridge, NY, 2005)
2. G. Rother, Y.B. Melnichenko, D.R. Cole, H. Frielinghaus, G.D. Wignall, J. Phys. Chem. C **111**, 15736 (2007)
3. Y.B. Melnichenko, G.D. Wignall, D.R. Cole, H. Frielinghaus, J. Chem. Phys. **124**, 204711 (2006)
4. W.L. Wu, Polymer **23**, 1907 (1982)
5. J. Goodisman, H. Brumberger, J. Appl. Cryst. **4**, 347 (1971)
6. S. Ciccariello, P. Riello, J. Appl. Cryst. **40**, 282 (2007)
7. A. Peterlin, Makromolek. Chem. **87**, 152 (1965)
8. P. Debye, H.R. Anderson, H. Brumberger, J. Appl. Cryst. **28**, 679 (1957)
9. K. Tajiri, K. Igarashi, T. Nishio, J. Non-Cryst. Solids **186**, 83 (1995)
10. G.D. Wignall, F.S. Bates, J. Appl. Crystallogr. **20**, 28 (1987)
11. Y.B. Melnichenko, G.D. Wignall, J. Appl. Phys. **102**, 021101 (2007)
12. R. Humauyn, D.L. Tomasko, AIChE J. **46**, 2065 (2000)
13. W. Gao, D. Butler, D.L. Tomasko, Langmuir **20**, 8083 (2004)
14. M.S. Schneider, J.D. Grunwaldt, A. Baiker, Langmuir **20**, 2890 (2004)
15. T.A. Steriotis, K.L. Stefanopoulos, A.C. Mitropoulos, N.K. Kanellopoulos, A. Hoser, M. Hofmann, Appl. Phys. **A74**, S1333 (2002)
16. T.A. Steriotis, K.L. Stefanopoulos, N.K. Kanellopoulos, A.C. Mitropoulos, A. Hoser, Colloid Surf. **A241**, 239 (2004)
17. A.P.Y. Wong, M.H.W. Chan, Phys. Rev. Lett. **65**, 2567 (1990)
18. A.P.Y. Wong, S.B. Kim, W.I. Goldburg, M.H.W. Chan, Phys. Rev. Lett. **70**, 954 (1993)
19. R. Garcia, S. Scheidemantel, K. Knorr, M.H.W. Chan, Phys. Rev. **E68**, 056111 (2003)
20. T. Herman, J.R. Beamish, J. Low Temp. Phys. **126**, 661 (2002)
21. T. Herman, J.R. Beamish, J. Low Temp. Phys. **141**, 193 (2005)
22. T. Herman, J.R. Beamish, Phys. Rev. **B72**, 184202 (2005)
23. K. Kaneko, K. Murata, Adsorption **3**, 197 (1997)
24. R. Sakurovs, S. Day, S. Weir, G. Duffy, Int. J. Coal Geol. **73**, 250 (2008)
25. Y.B. Melnichenko, A.P. Radlinski, M. Mastalerz, G. Cheng, J. Rupp, Int. J. Coal Geol. **77**, 69 (2009)
26. A.P. Radlinski, T.L. Busbridge, E.M. Gray, T.P. Blach, G. Cheng, Y.B. Melnichenko, D.J. Cookson, M. Mastalerz, J. Esterle, Langmuir **25**, 2385 (2009)
27. E. Hoinkis, Part. Part. Syst. Charact. **21**, 80 (2004)